ACES

DOI: 10.1002/ajoc.201402238

ASIAN JOURNAL OF ORGANIC CHEMISTRY
Full Paper

Rotaxanes

Light-Controlled [3]Pseudorotaxane Based on Tetrasulfonated 1,5-Dinaphtho-32-Crown-8 and α-Cyclodextrin

Jun Wang,[a] Ying-Ming Zhang,[a] Xu-Jie Zhang,[a] Xiao-Jun Zhao,*[b] and Yu Liu*[a]

Abstract: We developed the synthesis of a multicomponent molecular machine by employing the inclusion complex of an azobenzene-containing pyridinium salt (**G1**) with α-cyclodextrin (α-CD) and tetrasulfonated 1,5-dinaphtho-32-crown-8 (DNC) in water. The interconversion of the heterowheel *trans*-**G1**·DNC·α-CD [3]pseudorotaxane into *cis*-**G1**·DNC [2]pseudorotaxane was modulated by the photoinduced isomerization of the azobenzene moiety accompanied by the release of α-CD from the molecular axle. In control experiments, the azobenzene center of the bis(pyridinium)-modified azobenzene (**G2**) could not be isomerized in the presence of DNC and α-CD. Only polymeric aggregates were obtained with the **G2**·DNC·α-CD system, which indicates that the inclusion complex with α-CD and the electrostatic attraction with DNC are crucial to govern the reversible photoswitchable process. This work may provide a method to induce conformational changes of supramolecular assemblies that have multiple macrocyclic receptors.

Introduction

Artificial molecular machines, which self-assemble from discrete functional components and can carry out machine-like motions in response to external stimuli, have attracted considerable attention in recent years, because they can provide practical superiority in nanotechnology and materials sciences.[1] Consequently, considerable effort has been devoted to the development of advanced molecular machines with new functionality and good operability, such as a molecular switch, a molecular elevator, a molecular brake, and molecular scissors.[2] Among the numerous chromophores in the synthesis of molecular machines, the photochromic azobenzene derivatives, which can undergo a reversible *trans–cis* isomerization upon light irradiation, have broad potential for applications in various fields.[3] At the interface of photochemistry and supramolecular chemistry, the azobenzene group can act as a recognition site and be encapsulated by many different macrocycles, such as cyclodextrin,[4] calixarene,[5] pillararene,[6] and cucurbituril.[7] For instance, Harada and co-workers reported a photoswitchable gel assembly system that operated through the selective binding of azobenzene with α- and β-cyclodextrins (α- and β-CDs), which may be promising in the production of stimulus-responsive materials on a macroscopic scale.[8] Moreover, Huang and Liu et al. utilized azobenzene isomers to construct a pillar[6]arene-based binary complex, which led to a reversible photocontrolled interconversion between irregular and vesicle-like aggregates.[9]

Through quantitative analysis of crystallographic data and microcalorimetric titration results, our group has demonstrated that tetrasulfonatocrown ethers, as negatively charged receptors with a π-aromatic cavity, can form stable 1:1 complexes with various electron-deficient aromatic substrates through electrostatic attractions, π–π aromatic stacking, and hydrogen-bonding interconnections.[10] Our systematic work has also revealed that the equilibrium association constants of tetrasulfonatocrown ethers with dicationic bipyridiniums, pyromellitic and naphthalene diimides, and diquaternary salts are in the range from 10^5 to 10^8 M^{-1} orders of magnitude in water, which makes the water-soluble crown ether an ideal candidate for the construction of multicomponent molecular machines.

Herein, by combining the molecular binding characteristics of water-soluble crown ethers and the superior photochemical properties of azobenzene derivatives, we have developed the synthesis of a multicomponent [3]pseudorotaxane by employing the molecular recognition of azobenzene-containing pyridinium salt (**G1**) with α-cyclodextrin and tetrasulfonated 1,5-dinaphtho-32-crown-8 (DNC). The [3]pseudorotaxane of *trans*-**G1**·DNC·α-CD can be conveniently obtained by the molecular

[a] *J. Wang, Y.-M. Zhang, X.-J. Zhang, Y. Liu*
Department of Chemistry
State Key Laboratory of Elemento-Organic Chemistry
Collaborative Innovation Center of Chemical Science and Engineering (Tianjin), Nankai University
Tianjin 300071 (P. R. China)
E-mail: yuliu@nankai.edu.cn

[b] *X.-J. Zhao*
Key Laboratory of Inorganic-Organic Hybrid Functional Material Chemistry
Ministry of Education
Tianjin Key Laboratory of Structure and Performance for Functional Molecules, College of Chemistry
Tianjin Normal University
Tianjin 300387 (P. R. China)
E-mail: xiaojun_zhao15@163.com

Supporting information for this article is available on the WWW under http://dx.doi.org/10.1002/ajoc.201402238.

This manuscript is part of a special issue on molecular level devices and machines. Click here to see the Table of Contents of the special issue.

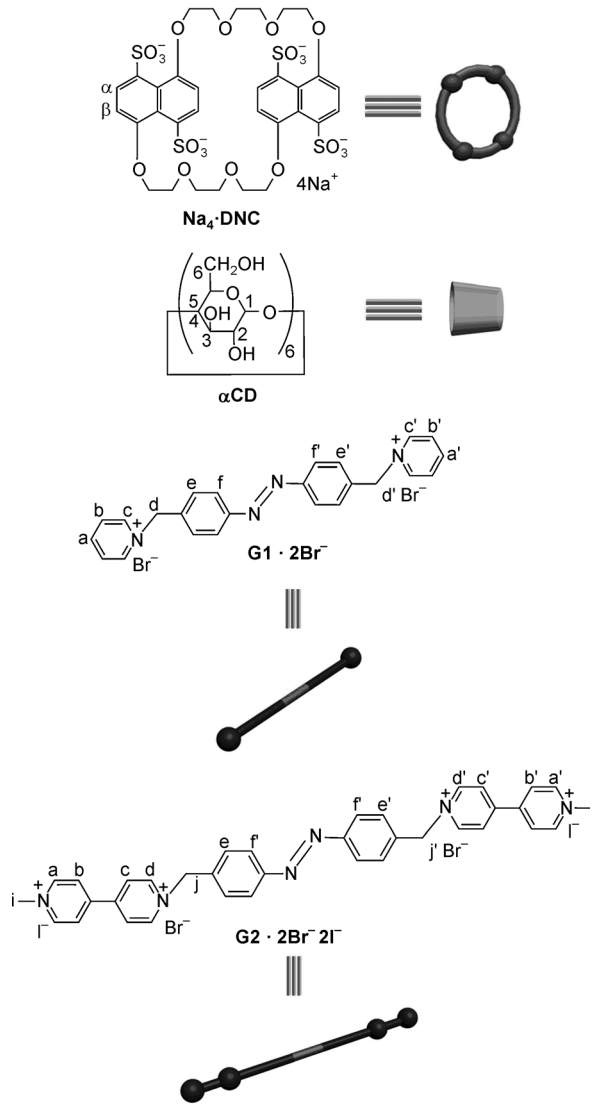

Scheme 1. Chemical structures and proton designations of Na_4·DNC, α-CD, **G1**·2Br^-, and **G2**·2Br^-·2I^-.

binding complementarity of the crown ether and α-CD. In addition, *trans*-**G1**·DNC·α-CD [3]pseudorotaxane can be further reversibly switched to *cis*-**G1**·DNC [2]pseudorotaxane upon photoirradiation. Interestingly, the motion of the macrocyclic host in [3]pseudorotaxane exhibits a guest-mediated response, that is, once the azobenzene guest is modified with the doubly-charged bis(pyridinium) terminal groups, instead of the singly-charged pyridinium units, the photoisomerization of *trans*-azobenzene can no longer be converted into the *cis* isomer in the presence of DNC and α-CD. The structural illustrations of DNC and α-CD as wheel molecules and **G1** and **G2** as axle molecules are shown in Scheme 1.

Results and Discussion

Formation of G1·DNC [2]Pseudorotaxane

The binding manner and stoichiometry of a spontaneous self-assembly process that involves discrete components should be confirmed.[11] Thus, ^{1}H NMR titration experiments were preliminarily performed in D_2O upon the gradual addition of DNC to a fixed concentration of **G1**. As shown in Figure S7 (Supporting Information), the proton signals of the axle molecule **G1** split into six groups, most of which (H_a–H_e and $H_{a'}$–$H_{e'}$) underwent a dramatic complex-induced upfield shift, whereas $H_{f,f'}$ moved in the opposite direction upon complexation with DNC. These phenomena indicate that the azobenzene center of **G1** is located in the cavity of DNC, which leaves the pyridinium moiety and the peripheral protons in the shielding area of the naphthalene moieties of DNC.[6,10] Moreover, the binding stoichiometry was explored by the tangent method[12] and Job plot analysis, in which the inflection point was found at the host-guest molar ratio of 1.0 (Figures 1a and S8, Supporting Information). The combination of the 1:1 binding stoichiometry with the aforementioned ^{1}H NMR titration results confirmed that axle guest **G1** is threaded into the crown ether ring of DNC to form a [2]pseudorotaxane in aqueous solution.

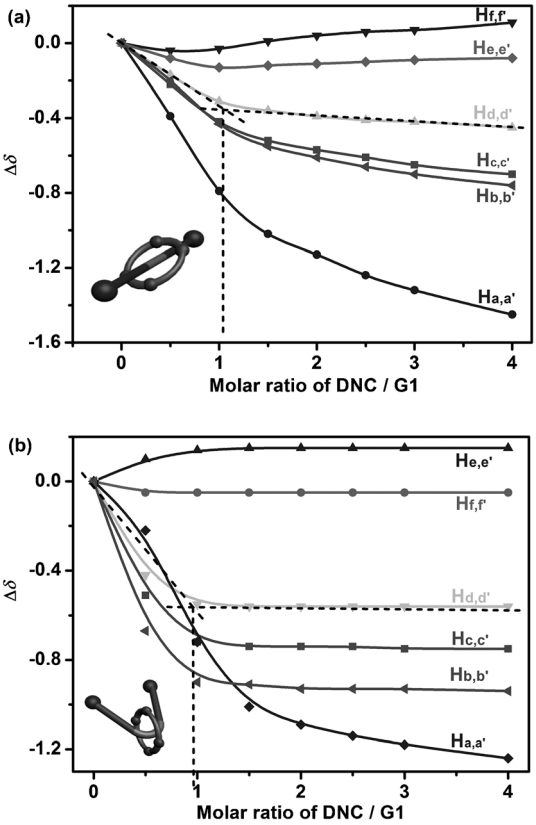

Figure 1. Plots of the changes in the chemical shift ($\Delta\delta$, ppm) of the protons in (a) *trans*-**G1** versus [DNC] in D_2O at 25 °C ([G1] = 2.0 mM) and (b) *cis*-**G1** versus [DNC] in D_2O at 25 °C ([G1] = 2.0 mM). Inset: inclusion binding modes of DNC with *trans*- and *cis*-**G1**, respectively.

The formation of G1·DNC [2]pseudorotaxane was further evaluated by isothermal titration calorimetry (ITC) experiments, which provided a strong association constant [$K = (1.51 \pm 0.08) \times 10^5\ M^{-1}$] and reliable thermodynamic parameters within reasonable experimental error ($\Delta G^\circ = -29.56 \pm 0.13$ kJ mol^{-1}, $\Delta H^\circ = -27.79 \pm 0.45$ kJ mol^{-1}, and $T\Delta S^\circ = 1.77 \pm 0.32$ kJ mol^{-1},

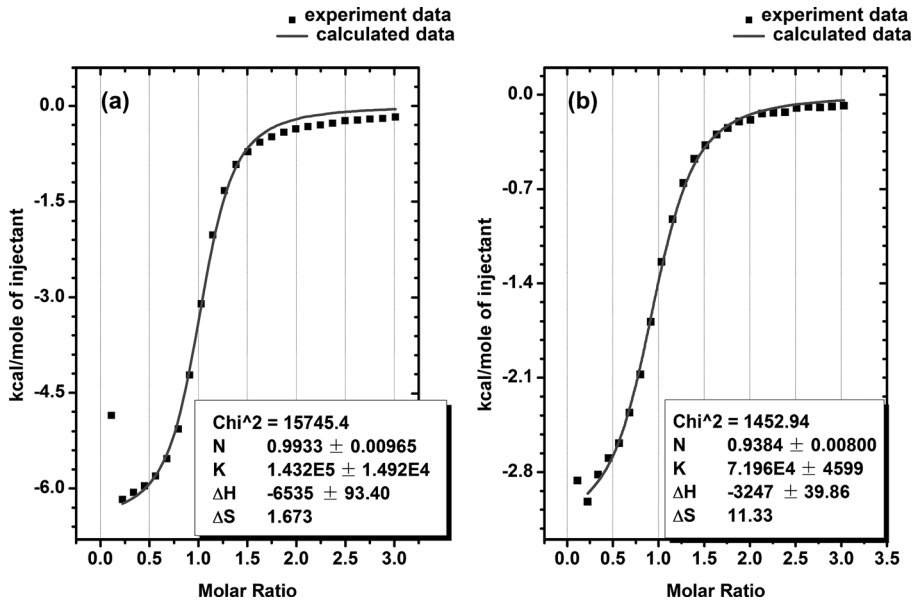

Figure 2. ITC curves for the complexation of (a) *trans*-**G1** with DNC and (b) *trans*-**G1**·α-CD with DNC in water at 25.00 °C.

Figures 2a and S9, Supporting Information). These results imply that the hydrogen-bonding interconnection and π-stacking interaction lead to a negative enthalpy change, and the ion-ion electrostatic attraction makes the positive contribution to the enthalpy change in the intermolecular binding process of **G1** with DNC.[10,13] In addition, direct evidence in support of the formation of G1·DNC [2]pseudorotaxane came from the ESI-MS spectra, in which the peaks at $m/z = 615.11$ and 1231.22 could be assigned to $[DNC+G1]^{2-}$ and $[DNC+G1+H]^{-}$, respectively (Figure S10, Supporting Information).

Interconversion of DNC with *cis*- and *trans*-G1

Because we identified the photochemical properties of **G1** in a previous work,[14] we expected that the [2]pseudorotaxane of *trans*-**G1**·DNC could be converted into *cis*-**G1**·DNC upon the photoinduced isomerization of the azobenzene group. As shown in Figure 3, the proton signals of *cis*-**G1** could be readily distinguished from its *trans* isomer within the NMR timescale after irradiation at 365 nm for 30 min. The chemical shift changes ($\Delta\delta$) of the *trans*- and *cis*-azobenzene moieties in the **G1**·DNC complexes exhibited a similar tendency, except that one of the $H_{e,e'}$ signals in *cis*-**G1** shifted downfield, which suggests that these protons were more conducive to form the C–H···O hydrogen bonds with the polyether chains of DNC. In comparison to free **G1**, the axle molecule *trans*-**G1** in [2]pseudorotaxane was accordingly converted into the *cis* isomer in a ratio of 60:40 *trans*/*cis* at the photostationary state. This result reveals that the complexation with the water-soluble crown ether did not make a tremendous impact on the photochemical properties of the azobenzene group in **G1**. Meanwhile, the tangent method and the Job plots further demonstrated that the **G1**·DNC complex maintained a 1:1 binding stoichiometry after irradiation at 365 nm (Figures 1b and S11, Supporting Information). The peak at $m/z = 1253.19$ for $[G1+DNC+Na]^{-}$ was also found in the ESI-MS spectra after photoirradiation, which indicates the existence of the [2]pseudorotaxane structure in solution (Figure S12, Supporting Information). More gratifyingly, *cis*-**G1**·DNC can revert back into *trans*-**G1**·DNC [2]pseudorotaxane as the predominant species upon irradiation with visible light at 450 nm (Figure S13, Supporting Information). Therefore, the reversible interconversion between *trans*-**G1**·DNC and *cis*-**G1**·DNC can be effectively achieved by the photoirradiation of the azobenzene unit, as described in Scheme 2.

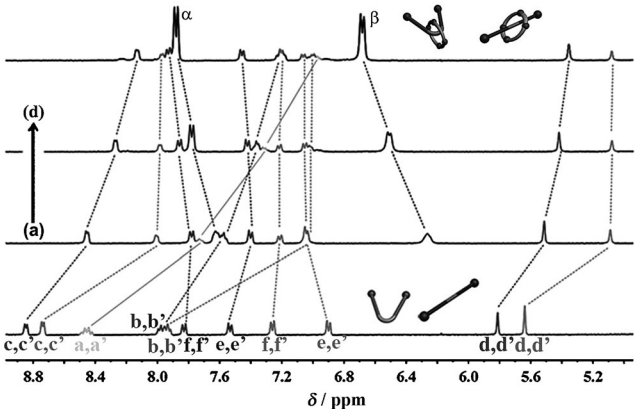

Figure 3. Partial ^{1}H NMR spectra (400 MHz, D_2O, 25 °C) of (a) **G1**, (b) **G1** in the presence of 1.0, (c) 2.0, and (d) 4.0 equiv. of DNC after irradiation at 365 nm for 30 min ([G1] = 2.0 mM). Black and dark grey labels refer to the *trans* and *cis* forms of **G1**, respectively.

To further investigate the photoswitchable process of DNC with *trans*- and *cis*-**G1**, a UV/vis spectroscopic investigation was carried out in water. Upon irradiation of the *trans*-**G1**·DNC solution at 365 nm, the band at 321 nm, which corresponds to the π–π* transition, sharply decreased, whereas the n–π* band at 425 nm gradually increased (Figure 4a). The association of **G1** with DNC can induce a change in the strength of absorption in the range of 270–380 nm, which is different from the spectral sum of the individual components (Figure S14, Supporting Information). In contrast, when the *trans*-**G1**·DNC solution was exposed at 450 nm, the spectral changes shifted in the opposite direction, and the spectroscopic features returned to the original state, indicating the regeneration of *trans*-**G1**·DNC [2]pseudorotaxane (Figure 4b). It is noteworthy that this photoswitchable process can be easily recycled several

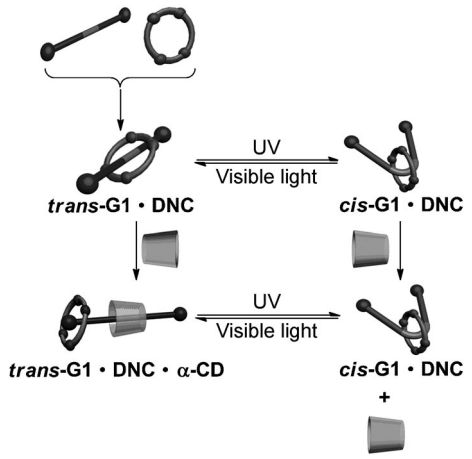

Scheme 2. Interconversion process of different types of pseudorotaxanes with DNC and α-CD in water.

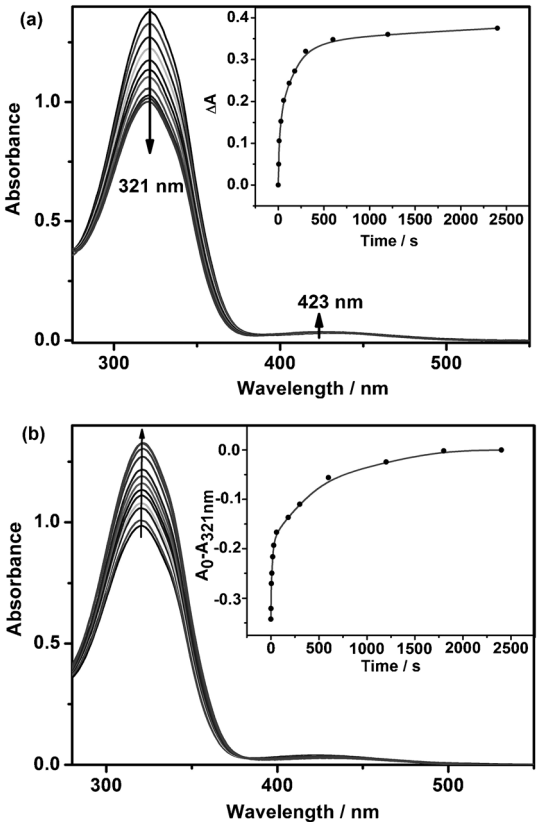

Figure 4. (a) UV/vis absorption spectra of *trans*-**G1**·DNC [2]pseudorotaxane after irradiation at 365 nm in water and (b) the same solution as (a) after irradiation with visible light at 450 nm. Inset: changes in absorbance at 321 nm versus irradiation time ([**G1**] = [DNC] = 0.03 mM, 25 °C).

times upon alternate exposure to UV and visible light (Figure S15, Supporting Information, inset).

Formation of Inclusion Complex G1·α-CD

It has been proven that an inclusion complex can form between azobenzene and α-CD in a pseudorotaxane fashion, and the threading and dethreading process can be conveniently modulated by the photoisomerization of azobenzene.[4,15] In our case, most of the signals from the azobenzene protons of **G1** had an obvious complex-induced downfield shift, which indicates that the *trans* isomer of **G1** is encapsulated in the cavity of α-CD (Figure S16a and b, Supporting Information). Comparatively, some new proton signals assigned to the *cis* isomer of the azobenzene group appeared when the sample was irradiated at 365 nm, and the *trans*-**G1**·DNC complex was produced upon continuous irradiation at 450 nm (Figure S16c and d, Supporting Information). In the rotating-frame Overhauser effect spectroscopy (ROESY) experiment, the signals from both $H_{f,f'}$ and $H_{e,e'}$ in *trans*-**G1** displayed clear nuclear Overhauser enhancement (NOE) cross-peaks with the interior protons of the α-CD cavity (peaks A and B in Figure S17, Supporting Information). In addition, the ITC study of the complexation of *trans*-**G1** with α-CD gave the relevant thermodynamic parameters and a relatively strong binding affinity ($K = 1.40 \times 10^4\ M^{-1}$, Figure S18, Supporting Information). With the benefit of the superior photochromic properties of azobenzene, the reversible photophysical behaviors of the **G1**·α-CD complex could be achieved under commutative irradiation at 360 and 450 nm (Figures S19 and S20, Supporting Information). Similar to the **G1**·DNC [2]pseudorotaxane, these results demonstrate that the inclusion complex between axle guest **G1** and macrocyclic host α-CD can also be reversibly modulated in a photoresponsive manner.[4a–c,16]

Formation of Heterowheel *trans*-G1·DNC·α-CD [3]Pseudorotaxane

With **G1**·DNC [2]pseudorotaxane and the inclusion complex **G1**·α-CD in hand, we envisioned that the formation of the **G1**·α-CD host-guest complex could influence the binding mode of **G1**·DNC [2]pseudorotaxane and then trigger conformational changes in the ternary complex of **G1**·DNC·α-CD. To test this conjecture, ^{1}H NMR spectroscopic titrations were performed with and without the added α-CD (Figure 5). Interestingly, when 1–3 equiv. of α-CD were gradually added to the *trans*-**G1**·DNC solution, all of the proton signals of **G1** were split into two groups, which suggests that α-CD was involved in the formation of an inclusion complex with **G1** through a hydrophobic interaction (Figure 5b–d). Meanwhile, upon complexation with α-CD, the proton signals of one pyridinium group ($H_{a'}$–$H_{c'}$) shifted upfield, whereas the remainder of the aromatic protons of **G1**·DNC (H_a–H_d, $H_{e,e'}$–$H_{f,f'}$) were completely restored to their original state. These phenomena indicate that the molecular symmetry of *trans*-**G1**·DNC [2]pseudorotaxane is broken by the association with α-CD, that is, α-CD competitively occupies the azobenzene moiety and then impels the crown ether ring to move from the aromatic center to a pyridinium terminal group. Moreover, as discerned from the ^{1}H ROESY spectrum of *trans*-**G1**·DNC·α-CD in Figure 6, cross-peaks A were assigned to the NOE correlation between the azobenzene center ($H_{f,f'}$ and $H_{e,e'}$) and the cavity of α-CD (H_3 and H_5), and cross-peaks B and C originated from the intermolecular communication between the axle ($H_{b',d}$) and aromatic protons

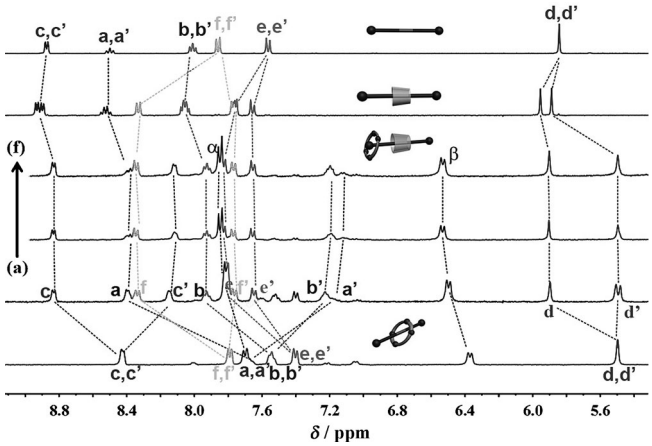

Figure 5. Partial ^{1}H NMR spectra (400 MHz, D_2O, 25 °C) of (a) *trans*-**G1**·DNC, (b) *trans*-**G1**·DNC in the presence of 1 equiv. of α-CD, (c) *trans*-**G1**·DNC in the presence of 2 equiv. of α-CD, (d) *trans*-**G1**·DNC in the presence of 3 equiv. of α-CD, (e) **G1** in the presence of 2 equiv. of α-CD, and (f) free **G1** ([**G1**] = [DNC] = 2.0 mM).

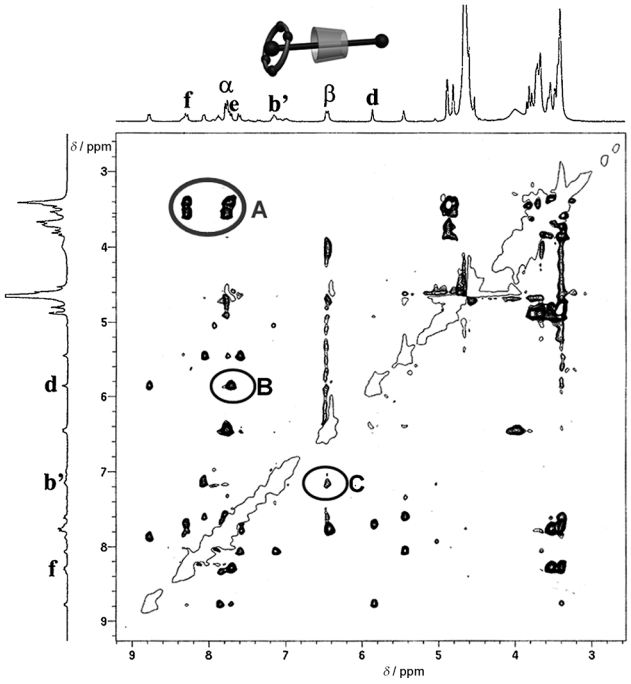

Figure 6. ^{1}H ROESY spectrum of *trans*-**G1**·DNC·α-CD in D_2O at 25 °C.

of DNC ($H_{\alpha,\beta}$). In addition, the peak at $m/z = 1170.91$ could be assigned to $[G1+\alpha\text{-CD}+DNC+Na+Br+2H_2O]^{2-}$ in the ESI-MS spectrum (Figure S21, Supporting Information). By combining these characterization results, we can reasonably infer that two different types of macrocyclic receptors, α-CD and the tetrasulfonated crown ether, can concurrently reside around the axle molecule of the azobenzene-containing pyridinium salt.

Although the location of DNC changed with respect to axle molecule **G1** upon addition of α-CD, it maintained the 1:1 binding stoichiometry between **G1** and DNC, which would facilitate the eventual formation of a heterowheel pseudo[3]rotaxane (Figure S22, Supporting Information). In addition, in comparison to the *trans*-**G1**·DNC system, the *K* value of *trans*-**G1**·α-CD with DNC decreased to $7.20\times10^4\ M^{-1}$, probably because of the severe steric hindrance from α-CD around the pyridinium moiety, which would inhibit the electrostatic attraction with DNC (Figures 2b and S23, Supporting Information). Together, these observations imply that α-CD is a good candidate to induce the motion of crown ether ring from the hydrophobic center to the positively charged end group in molecular axle **G1**.

Interconversion between *trans*-G1·DNC·α-CD and *cis*-G1·DNC

Taking into consideration the photoactive azobenzene group in the [3]pseudorotaxane, we investigated the light-controlled behavior of **G1**·DNC·α-CD. As shown in Figure S24a (Supporting Information), a new set of signals resulted by irradiating the *trans*-**G1**·DNC·α-CD solution at 365 nm for 30 min, which corresponded to the characteristic signals of the *cis* isomer within **G1**·DNC. Compared with the ^{1}H NMR spectrum in Figure 3, we concluded that the *trans*-**G1**·DNC·α-CD [3]pseudorotaxane was partially converted into the *cis*-**G1**·DNC [2]pseudorotaxane along with the dissociation of the *trans*-azobenzene·α-CD complex. Moreover, after subsequent irradiation at 450 nm, the proton signals for *cis*-**G1**·DNC disappeared and gave rise to the regeneration of *trans*-**G1**·DNC·α-CD (Figure S24b, Supporting Information). As a result, because of the advantageous photochemical properties of azobenzene, a highly reversible conformational change in the transition from [3]pseudorotaxane to [2]pseudorotaxane can operate through the assembling/disassembling processes of the *trans*-/*cis*-azobenzene with α-CD (Figures S25 and S26, Supporting Information).

Interconversion Process of G2 with DNC and α-CD

Because the photoisomerization of the azobenzene unit is a crucial factor in governing the molecular binding behaviors with DNC and α-CD, we expect that the type of motion can be further manipulated by changing the guest molecular structure (e.g., the π-aromatic conjugation and charge density), as the binding selectivity of DNC to dicationic bis(pyridinium) guests is higher than that of singly-charged pyridinium ones.[10] Therefore, compound **G2** was synthesized to have bis(pyridinium) terminal groups, a greater π-conjugated system, and more positive charge numbers. As expected, the signals of $H_{e,e'}$ and $H_{f,f'}$ in **G2** displayed an obvious complex-induced chemical shift upon the addition of α-CD, which was similar to the **G1**·α-CD system (Figure S27b, Supporting Information). In addition, the NOE cross-peaks in the ^{1}H ROESY spectra further supported the formation of the host-guest inclusion complex of **G2**·α-CD (Figure S28, Supporting Information). These results demonstrate that the structural modification to have the bis(pyridinium) terminal groups did not affect the encapsulation of doubly-charged azobenzene within the cavity of α-CD.

However, in contrast to the **G1**·DNC [2]pseudorotaxane, some irregular coaggregation was observed in the equimolar mixture of DNC with **G2** at a higher concentrations, which ultimately resulted in broad and ill-defined signals in the ^{1}H NMR

spectra, even with 10% dimethyl sulfoxide (DMSO) as a cosolvent (Figure S27c, Supporting Information). The undesirable aggregation is mainly a result of the strong electrostatic attractions upon charge-neutralizing complexation in the **G2**·DNC system. Nevertheless, the exact binding stoichiometry could be detected in dilute solution by means of ESI-MS, in which the signal at $m/z = 1413.30$ was assigned to $[G2+DNC-H]^-$ (Figure S29, Supporting Information).

Subsequently, when DNC was mixed with the **G2**·α-CD complex in a 1:1 ratio, the signal at $m/z = 836.43$ could be assigned to $[G2+\alpha\text{-CD}+DNC+3\,Na+3\,H_2O]^{3+}$, which is indicative of the formation of the heterowheel **G2**·DNC·α-CD [3]pseudorotaxane (Figure S30, Supporting Information). Moreover, the NMR signals of the obtained [3]pseudorotaxane were drastically broadened, which was distinctive from the free axle molecule **G2** and its corresponding **G2**·α-CD complex with a simple peak pattern. This was presumably because of the formation of polymeric species in solution (Figure S27d, Supporting Information).[7b,17] The morphological information of this self-assembled nanoarchitecture was further obtained by the atomic force microscopy (AFM), in which the 1:1:1 mixture of **G2**·DNC·α-CD showed the presence of spherical nanoparticles with an average height that ranged from 1.5 to 9.0 nm (Figure S31a–c, Supporting Information). Along with these concentration-dependent behaviors in the microscopic investigation, we also found that the viscosity of the solution dramatically increased as the concentration of the **G2**·DNC·α-CD [3]pseudorotaxanes increased from 0.08 to 2.0 mM, which can provide additional evidence for the formation of aggregates in solution (Figure S32, Supporting Information).

Because of its molecular rigidity and positive charges, the molecular axle **G2** can isomerize with a relatively low conversion of approximately 50% (Figure S33, Supporting Information). However, as shown in Figure S34 (Supporting Information), when the dilute solution **G2**·DNC·α-CD was exposed to UV light, there was no noticeable change in the n–π* transition in the long wavelength region, and the absorbance was rather weak for the π–π* transition. Furthermore, no significant morphological change was observed in the AFM images upon irradiation at 365 nm. This indicates that the geometric configuration of the azobenzene center was stabilized by DNC and α-CD, which suppressed the photoinduced isomerization of azobenzene in **G2** (Figure S31d, Supporting Information). Combining these spectroscopic and microscopic investigation results, we deduced that the azobenzene group of **G2** was accommodated in the cavity of α-CD and that one of bis(pyridinium) terminal groups is encircled by DNC to form the [3]pseudorotaxane. The other positively charged group may intermolecularly communicate with the neighboring DNC molecules to form a polymeric aggregation through the strong electrostatic attraction between the bis(pyridinium) salts and sulfonate sites. The possible aggregation mode is proposed in Scheme 3.

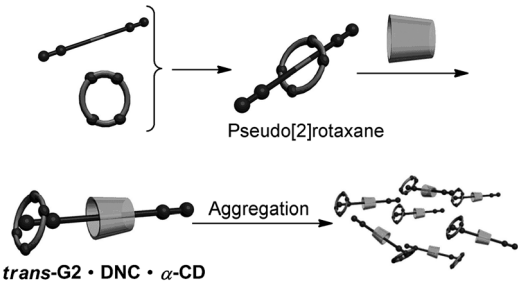

Scheme 3. Schematic illustration of supramolecular aggregation based on the heterowheel of **G2**·DNC·α-CD pseudo[3]rotaxane.

Conclusions

In summary, we have synthesized a light-controlled *trans*-**G1**·DNC·α-CD [3]pseudorotaxane through the supramolecular cooperativity of an azobenzene-pyridinium conjugate with two different types of macrocyclic receptors in aqueous solution. The formation of this ternary assembly is driven by the combination of the hydrophobic interaction of α-CD with *trans*-azobenzene and the electrostatic attraction between the tetrasulfonatocrown ethers and the singly-charged pyridinium salt. Notably, upon the photoisomerization of the azobenzene group from its *trans* to *cis* isomer, the α-CD unit is released from the molecular axle, and the crown ether ring slides from the pyridinium terminal group to the azobenzene group in the center. Moreover, the operation of this molecular machine can be controlled by the guest molecular structures. As investigated by spectroscopy and microscopic observations, the spatial arrangement of the individual components of the [3]pseudorotaxane is fixed by using the bis(pyridinium)-modified azobenzene as a reference guest, and the photoisomerization of the azobenzene can suppressed by the simultaneous incorporation of the water-soluble crown ether and α-CD. We anticipate that the realization of the effective complexation between azobenzene and the crown ether in this work can further provide strategies to develop more sophisticated molecular machines in water.

Experimental Section

Instrumentation and Methods

All chemicals were commercially available, and all experiments were performed at 25 °C and in deionized water, unless noted otherwise. The ^{1}H NMR spectra were recorded on a Bruker 400 MHz instrument, and D_2O was used as the NMR solvent. Chemical shifts were recorded in parts per million (ppm). The ^{1}H ROESY spectra were recorded in D_2O on a Bruker 300 MHz instrument. Absorption spectra were record on a Shimadzu UV-3600 spectrophotometer that was equipped with a PTC-348WI temperature controller. Mass spectrometry was performed on a Q-TOF LC–MS in the ESI mode. AFM images were recorded on an atomic force microscope (Veeco Company, Multimode, Nano IIIa). Viscometer measurements were carried out in deionized water on a SCHOTT-Ubbelohde microcapillary viscometer (DIN 53810, 0.40 mm inner diameter).

Isothermal Titration Calorimetry (ITC)

A thermostatted and fully computer-operated isothermal calorimetry instrument (VP-ITC, purchased from MicroCal, Northampton, MA) was used for all microcalorimetric experiments to provide the binding constants (*K*) and thermodynamic parameters. The dilution enthalpies determined in control experiments were subtracted

from the enthalpies that were measured in the titration experiments to obtain the net heat of the reaction. All thermodynamic parameters reported in this work were obtained by using the "one set of binding sites" model. Two independent titration experiments were performed to afford self-consistent parameters, which were used to calculate the average values.

Photoirradiation

The irradiation light source for photoisomerization was a high-pressure mercury lamp with an optical fiber (CEL-M500, purchased from ZhongJiaoJinYuan Scientific & Technological Co., Ltd., China). The two band-pass filters were of the wavelengths 365 ± 15 and 450 ± 15 nm, respectively. Sample solutions of different concentrations were irradiated by UV or visible light for further measurements.

Synthesis

The water-soluble crown ether DNC[10b] and the precursor of 1,2-bis[4-(bromomethyl)phenyl]diazene[18] (BBPD) were synthesized according to previous reports. The characterizations of **G1** and **G2** are listed in Figures S1 through S6 in the Supporting Information.

Synthesis of G1: The precursor compound BBPD (184 mg, 0.5 mmol) was dissolved in anhydrous *N*,*N*-dimethylformamide (DMF, 5 mL) at 90 °C. When the raw material was dissolved completely, pyridine (118.5 mg, 1.5 mmol) was added in portion and, the resulting mixture was then stirred for 24 h. The hot reaction mixture was filtered, and the solid product was washed with DMF. After vacuum drying, a yellow power was obtained (96% yield). ^{1}H NMR (400 MHz, D_2O): $\delta = 8.87$ (d, $H_{c,c'}$, 4H), 8.50 (t, $H_{a,a'}$, 2H), 8.01 (t, $H_{b,b'}$, 4H), 7.86 (d, $H_{f,f'}$, 4H), 7.56 (d, $H_{e,e'}$, 4H), 5.84 ppm (s, $H_{d,d'}$, 4H); ^{13}C NMR (100 MHz, D_2O): $\delta = 152.6$, 146.2, 144.5, 136.1, 130.1, 128.5, 123.4, 63.9 ppm; MS (ESI): *m*/*z*: calcd for $C_{24}H_{22}N_4Br_2$: 183.09 $[M-2Br]^{2+}$; found: 183.09.

Synthesis of G2: Guest compound **G2** was synthesized by using a similar procedure to that of **G1**. ^{1}H NMR (400 MHz, D_2O): $\delta = 9.13$ (d, $H_{d,d'}$, 4H), 8.95 (d, $H_{a,a'}$, 4H), 8.48 (d, $H_{b,b'}$, 4H), 8.42 (d, $H_{c,c'}$, 4H), 7.90 (d, $H_{f,f'}$, 4H), 7.63 (d, $H_{e,e'}$, 4H), 5.96 (s, $H_{j,j'}$, 4H), 4.40 ppm (s, $H_{i,i'}$, 6H); ^{13}C NMR (100 MHz, D_2O): $\delta = 152.7$, 150.6, 149.6, 146.3, 145.7, 135.6, 130.4, 127.3, 126.8, 123.6, 64.2, 48.5 ppm; MS (ESI): *m*/*z*: calcd for $C_{36}H_{34}Br_2I_2N_6$: 274.13 $[M-2Br-2I-2H]^{2+}$; found: 274.12.

Acknowledgements

We thank the 973 Program (2011CB932502) and the NNSFC (91227107 and 21102075) for financial support.

Keywords: α-cyclodextrin · isomerization · molecular devices · rotaxanes · supramolecular chemistry

[1] a) B. Lewandowski, G. De Bo, J. W. Ward, M. Papmeyer, S. Kuschel, M. J. Aldegunde, P. M. E. Gramlich, D. Heckmann, S. M. Goldup, D. M. D'Souza, A. E. Fernandes, D. A. Leigh, *Science* **2013**, *339*, 189–193; b) J. Wang, B. L. Feringa, *Science* **2011**, *331*, 1429–1432; c) A. Harada, A. Hashidzume, H. Yamaguchi, Y. Takashima, *Chem. Rev.* **2009**, *109*, 5974–6023; d) E. R. Kay, D. A. Leigh, F. Zerbetto, *Angew. Chem. Int. Ed.* **2007**, *46*, 72–191; *Angew. Chem.* **2007**, *119*, 72–196; e) E. R. Kay, D. A. Leigh, *Nature* **2006**, *440*, 286–287; f) V. Fasano, M. Baroncini, M. Moffa, D. Iandolo, A. Camposeo, A. Credi, D. Pisignano, *J. Am. Chem. Soc.* **2014**, *136*, 14245–14254.

[2] a) J. D. Badjić, V. Balzani, A. Credi, S. Silvi, J. F. Stoddart, *Science* **2004**, *303*, 1845–1849; b) T. R. Kelly, M. C. Bowyer, K. V. Bhaskar, D. Bebbington, A. Garcia, F. Lang, M. H. Kim, M. P. Jette, *J. Am. Chem. Soc.* **1994**, *116*, 3657–3658; c) T. Muraoka, K. Kinbara, Y. Kobayashi, T. Aida, *J. Am. Chem. Soc.* **2003**, *125*, 5612–5613; d) H.-B. Cheng, H.-Y. Zhang, Y. Liu, *J. Am. Chem. Soc.* **2013**, *135*, 10190–10193.

[3] a) D. Patra, H. Zhang, S. Sengupta, A. Sen, *ACS Nano* **2013**, *7*, 7674–7679; b) S. K. M. Nalluri, B. J. Ravoo, *Angew. Chem. Int. Ed.* **2010**, *49*, 5371–5374; *Angew. Chem.* **2010**, *122*, 5499–5502; c) I. Tochitsky, M. R. Banghart, A. Mourot, J. Z. Yao, B. Gaub, R. H. Kramer, D. Trauner, *Nature Chem.* **2012**, *4*, 105–111; d) A. A. Beharry, G. A. Woolley, *Chem. Soc. Rev.* **2011**, *40*, 4422–4437; e) X. Wang, J. Huang, Y. Zhou, S. Yan, X. Weng, X. Wu, M. Deng, X. Zhou, *Angew. Chem. Int. Ed.* **2010**, *49*, 5305–5309; *Angew. Chem.* **2010**, *122*, 5433–5437; f) S. Yagai, A. Kitamura, *Chem. Soc. Rev.* **2008**, *37*, 1520–1529; g) V. Balzani, A. Credi, M. Venturi, *Chem. Soc. Rev.* **2009**, *38*, 1542–1550.

[4] a) X. J. Liao, G. S. Chen, X. X. Liu, W. X. Chen, F. E. Chen, M. Jiang, *Angew. Chem. Int. Ed.* **2010**, *49*, 4409–4413; *Angew. Chem.* **2010**, *122*, 4511–4515; b) H. M. D. Bandara, S. C. Burdette, *Chem. Soc. Rev.* **2012**, *41*, 1809–1825; c) R. Sun, C. Xue, X. Ma, M. Gao, H. Tian, Q. Li, *J. Am. Chem. Soc.* **2013**, *135*, 5990–5993; d) L. Peng, M. You, C. Wu, D. Han, I. Öçsoy, T. Chen, Z. Chen, W. Tan, *ACS Nano* **2014**, *8*, 2555–2561.

[5] a) T. Arimura, H. Kawabata, T. Matsuda, T. Muramatsu, H. Satoh, K. Fujio, O. Manabe, S. Shinkai, *J. Org. Chem.* **1991**, *56*, 301–306; b) X. Zhang, H. Zhao, D. Tian, H. Deng, H. Li, *Chem. Eur. J.* **2014**, *20*, 9367–9371.

[6] T. Ogoshi, K. Kida, T. Yamagishi, *J. Am. Chem. Soc.* **2012**, *134*, 20146–20150.

[7] a) H.-B. Cheng, Y.-M. Zhang, C. Xu, Y. Liu, *Sci. Rep.* **2014**, *4*, 4210–4215; b) J. del Barrio, P. N. Horton, D. Lairez, G. O. Lloyd, C. Toprakcioglu, O. A. Scherman, *J. Am. Chem. Soc.* **2013**, *135*, 11760–11763; c) C. Stoffelen, J. Voskuhl, P. Jonkheijm, J. Huskens, *Angew. Chem. Int. Ed.* **2014**, *53*, 3400–3404; *Angew. Chem.* **2014**, *126*, 3468–3472; d) F. Tian, D. Jiao, F. Biedermann, O. A. Scherman, *Nat. Commun.* **2012**, *3*, 1207; e) Y. Lan, Y. Wu, A. Karas, O. A. Scherman, *Angew. Chem. Int. Ed.* **2014**, *53*, 2166–2169; *Angew. Chem.* **2014**, *126*, 2198–2201.

[8] H. Yamaguchi, Y. Kobayashi, R. Kobayashi, Y. Takashima, A. Hashidzume, A. Harada, *Nat. Commun.* **2012**, *3*, 603.

[9] G. Yu, C. Han, Z. Zhang, J. Chen, X. Yan, B. Zheng, S. Liu, F. Huang, *J. Am. Chem. Soc.* **2012**, *134*, 8711–8717.

[10] a) L. Chen, Y.-M. Zhang, Y. Liu, *J. Phys. Chem. B* **2012**, *116*, 9500–9506; b) L. Chen, H.-Y. Zhang, Y. Liu, *J. Org. Chem.* **2012**, *77*, 9766–9773; c) L. Chen, Y.-M. Zhang, L.-H. Wang, Y. Liu, *J. Org. Chem.* **2013**, *78*, 5357–5363; d) Y.-M. Zhang, Z. Wang, L. Chen, H.-B. Song, Y. Liu, *J. Phys. Chem. B* **2014**, *118*, 2433–2441.

[11] S. Saha, J. F. Stoddart, *Chem. Soc. Rev.* **2007**, *36*, 77–92.

[12] H.-X. Zhao, D.-S. Guo, Y. Liu, *J. Phys. Chem. B* **2013**, *117*, 1978–1987.

[13] a) Y. Liu, X.-Y. Li, H.-Y. Zhang, C.-J. Li, F. Ding, *J. Org. Chem.* **2007**, *72*, 3640–3645; b) D. J. Hoffart, J. Tiburcio, A. de La Torre, L. K. Knight, S. J. Loeb, *Angew. Chem. Int. Ed.* **2008**, *47*, 97–101; *Angew. Chem.* **2008**, *120*, 103–107; c) A. L. Hubbard, G. J. E. Davidson, R. H. Patel, J. A. Wisner, S. J. Loeb, *Chem. Commun.* **2004**, 138–139; d) S. J. Loeb, *Chem. Soc. Rev.* **2012**, *41*, 1621–1636.

[14] H. Qian, D.-S. Guo, Y. Liu, *Asian J. Org. Chem.* **2012**, *1*, 155–159.

[15] a) D.-H. Qu, Q.-C. Wang, J. Ren, H. Tian, *Org. Lett.* **2004**, *6*, 2085–2088; b) H. Murakami, A. Kawabuchi, K. Kotoo, M. Kunitake, N. Nakashima, *J. Am. Chem. Soc.* **1997**, *119*, 9605–9606; c) X. Ma, D. Qu, F. Ji, Q. Wang, L. Zhu, Y. Xu, H. Tian, *Chem. Commun.* **2007**, 1409–1411; d) I. Tomatsu, A. Hashidzume, A. Harada, *J. Am. Chem. Soc.* **2006**, *128*, 2226–2227.

[16] a) D.-H. Qu, Q.-C. Wang, H. Tian, *Angew. Chem. Int. Ed.* **2005**, *44*, 5296–5299; *Angew. Chem.* **2005**, *117*, 5430–5433; b) H. Murakami, A. Kawabuchi, R. Matsumoto, T. Ido, N. Nakashima, *J. Am. Chem. Soc.* **2005**, *127*, 15891–15899.

[17] F. Wang, J. Zhang, X. Ding, S. Dong, M. Liu, B. Zheng, S. Li, L. Wu, Y. Yu, H. W. Gibson, F. Huang, *Angew. Chem. Int. Ed.* **2010**, *49*, 1090–1094; *Angew. Chem.* **2010**, *122*, 1108–1112.

[18] F. Bonardi, G. London, N. Nouwen, B. L. Feringa, A. J. M. Driessen, *Angew. Chem. Int. Ed.* **2010**, *49*, 7234–7238; *Angew. Chem.* **2010**, *122*, 7392–7396.

Received: November 6, 2014
Published online on January 15, 2015